Measurement of Transfer Constant for Butyl Acrylate Free-Radical Polymerization

Serge Maeder and Robert G. Gilbert*

School of Chemistry, University of Sydney, New South Wales 2006, Australia

Received January 15, 1998; Revised Manuscript Received April 27, 1998

ABSTRACT: Arrhenius parameters for the transfer constant to monomer (C_M) for the free-radical polymerization of butyl acrylate (BA) are determined by a combination of techniques. A seeded emulsion polymerization with conditions designed so that "zero−one" kinetics are obeyed, i.e., where entry of a radical into a particle causes instantaneous termination, such that transfer to monomer can be shown to be the dominant chain-stopping event. The seed comprised small polystyrene particles, which reduces the likelihood of chain transfer to polymer provided the polymer:monomer ratio is sufficiently low. Since the dominant chain-stopping events are then entry and transfer to monomer, C_M can then be obtained from the number molecular weight distribution for different initiator concentrations and conversions and isolating the component due to transfer to monomer. The transfer constant so obtained, over the temperature range 50−72 °C, fits $C_M = (0.016 \pm 0.003) \exp(-(15.2 \pm 0.6)\ \text{kJ mol}^{-1}/RT)$.

Introduction

The transfer constants to monomer (C_M) for free-radical polymerizations of acrylates have proved hard to measure: for example, literature data for C_M for methyl acrylate show a very wide variation,[1] while the only Arrhenius data for butyl acrylate reported thus far[2] suggest that the activation energy was the same as that for propagation, an implication that seems unlikely from consideration of the different natures of the transition states involved.[3] The reasons for these problems are not apparent but may include the presence of trace impurities which act as chain transfer agents and/or chain transfer to polymer (which is known to be quite likely for such monomers[4,5]). We here develop a new combination of techniques for determining the transfer constant to monomer for such difficult systems and apply it to butyl acrylate (BA).

The traditional means of obtaining the transfer constant to monomer, C_M, is the Mayo method, whereby $\langle M_n \rangle$ (the number-average molecular weight) is plotted against $[I]/R_p$ (where [I] is the initiator concentration and R_p the polymerization rate). However, this technique has a number of difficulties, discussed elsewhere.[6,7] These problems essentially arise because it is often difficult to determine an accurate $\langle M_n \rangle$ in the limit where transfer to monomer is the dominant chain-stopping event.

A relatively new method for obtaining transfer constants has been suggested, which utilizes information contained in the number molecular weight distribution (MWD).[6−13] The number MWD, $P(M)$, the number of chains with molecular weight M, is obtained relatively easily from the MWD produced in GPC, as discussed below, and under certain circumstances, this can be shown to have a region wherein $\ln P(M) \propto C_M M/M_0$, where M_0 is the molecular weight of monomer. This method requires that one can identify a region in the full MWD where chain stoppage is dominated by transfer to monomer (rather than the requirement of the Mayo method that one can extrapolate such that the *average* molecular weight is dominated by transfer to monomer). However if *termination* is extensive, this may not be possible in practice: for example, while in principle it is always possible to reach the transfer-dominated limit by reducing radical flux, it may not be possible to have sufficient polymer formed at appropriate molecular weights to obtain an accurate GPC signal.

The combination of techniques used here to overcome these problems are as follows. Polymerization is in a seeded emulsion polymerization system, whereby the conditions are chosen such that "zero−one" kinetics[9] are obeyed: that is, entry of a radical into a particle already containing a growing radical results in very rapid termination; this ensures that termination is unlikely between two long growing chains, and as is well-known, this reduction in termination (due to compartmentalization) means that a relatively high polymerization rate can be achieved and thus adequate amounts of polymer formed. Zero−one conditions can be usually (but not always[8,9]) obtained with suitably small particles, with the additional requirement that seeded polymerization occurs in the absence of secondary particle formation. The desired second-stage MWD can then be obtained by subtracting the seed MWD from the cumulative MWD of seed and formed polymer. A related method has been used by Schweer *et al.*[14] to obtain transfer constants in a strongly compartmentalized system, viz., a styrene microemulsion polymerization.

Because it is often difficult to obtain a suitable monodisperse latex of requisite particle size, the seed can be of a different polymer from that in the second-stage growth: so-called "hetero-seeded" emulsion polymerization.[15] Now, this would eventually result in phase separation of the second-stage polymer; however, if polymerization is only carried out to low conversion, then the unpolymerized monomer acts as compatibilizer between the two different polymers so that phase separation can be avoided. In the present case, the seed latex was chosen to be polystyrene (PS), which has the additional advantage of minimizing the likelihood of chain branching to polymer with the newly polymerized butyl acrylate (since most of the polymer in the system is polystyrene, which has a low rate of chain transfer

* Author to whom correspondence should be addressed.

S0024-9297(98)00051-5 CCC: $15.00
Published on Web 06/25/1998

to polymer even with reactive radicals such as those from BA).

Background Theory and Application to Butyl Acrylate

Molecular Weight Distributions in a Zero−One System. In a zero−one system, by definition the only chain-stopping events are entry and transfer to monomer (transfer to chain-transfer agent is trivially included, but omitted here for simplicity); transfer to polymer is assumed to be negligible. The instantaneous number MWD is then given by[10,16]

$$\ln P(M) = (\text{arbitrary constant}) - \frac{\rho_{\text{initiator}} + \rho_{\text{thermal}} + k_{\text{tr}}[\text{M}]_{\text{p}}}{k_{\text{p}}[\text{M}]_{\text{p}}} \frac{M}{M_0} \quad (1)$$

where the arbitrary constant is given by a convenient normalization (e.g., to conversion), $\rho_{\text{initiator}}$ and ρ_{thermal} are, respectively, the pseudo-first order rate coefficients for entry into the particle of a radical arising directly from initiator and from "background thermal" (spontaneous) sources,[17−19] k_{tr} and k_{p} are, respectively, the rate coefficients for transfer to monomer and propagation, and $[\text{M}]_{\text{p}}$ is the concentration of monomer in the latex particle.

Equation 1 shows that the transfer constant ($k_{\text{tr}}/k_{\text{p}}$) can be obtained from the slope of a plot of ln $P(M)$ against M for a system following zero−one kinetics, in the limit of low radical flux. If it can be shown that background thermal (spontaneous) polymerization is unimportant and if this slope is independent of initiator concentration, then this slope is $(k_{\text{tr}}/k_{\text{p}})M_0$.

The instantaneous number MWD is related to the GPC trace as follows. The GPC signal at elution volume V_{el} is related to the *cumulative* number MWD, $\bar{P}(M)$, by:[10,20]

$$\bar{P}(M) = \frac{G(V_{\text{el}})}{M} \left.\frac{\text{d}V_{\text{cal}}}{\text{d}M}\right|_{V_{\text{cal}}(M)=V_{\text{el}}} \quad (2)$$

where the function $V_{\text{cal}}(M)$ is the GPC calibration curve. In the common case of a linear calibration (i.e., $V_{\text{cal}}(M) = a + b \log M$), then one has simply

$$\bar{P}(M) = \begin{pmatrix}\text{normalization}\\ \text{constant}\end{pmatrix} \frac{G(V_{\text{el}})}{M^2} \quad (3)$$

In turn, the instantaneous distribution can be obtained from the cumulative distribution by subtracting appropriately normalized[21] cumulative distributions obtained at closely spaced conversions.

It is convenient to report GPC traces as the so-called GPC distribution, $w(\log M)$, wherein effects in the GPC trace due to nonlinearities in the calibration are removed:[20]

$$w(\log M) = G(V_{\text{el}}) \frac{\text{d}V_{\text{cal}}}{\text{d}(\log M)} \quad (4)$$

Choosing Conditions for the System to be Zero−One. It is necessary to specify how conditions can be chosen so that zero−one kinetics is obeyed. This issue has been addressed previously,[9,22] but we present here a modification and improvement of this earlier work. The definition of a zero−one system (that an entering radical causes very rapid termination) can be re-stated, in the context of MWDs, as being that entry of a radical into a particle which already contains a growing chain will lead to a high probability of termination before significant new polymer is formed. In quantifying this, account must be taken of the fact that the rate coefficient for termination in a latex particle is highly likely to depend on the lengths of each chain,[10,21,23−28] especially since the polymer concentration in a latex particle is always well above c^{**}, the concentration where chain entanglement sets in.[29] Moreover, for low degrees of polymerization, the propagation rate coefficient can also be chain-length dependent.[30,31]

Consider the fates which a radical entering a particle already containing a growing chain may undergo. Now, the preexisting radical will be of a high degree of polymerization (since degrees of polymerization of non-growing chains in emulsion polymerizations are typically on the order of 10^4). There is considerable evidence that termination in systems involving a long and a short radical is dominated by the diffusion of the smaller, more mobile species,[10,21,25−28,32−34] and so we denote by $k_{\text{t}}^{i\text{L}}$ the requisite termination rate coefficient between a radical of degree of polymerization i which has entered (and may have propagated a few steps) and a long radical, where L refers to "long". The propagation rate coefficient of an i-meric radical is denoted by k_{p}^{i}. Because only relatively short mutual growth times of the two chains are anticipated, transfer can be ignored when looking at the probability of the new radical propagating to a significant length before termination. The propagation rate is $k_{\text{p}}^{i}[\text{M}]_{\text{p}}$, while the rate of termination in a particle already containing a single long growing radical is $k_{\text{t}}^{i\text{L}}/N_{\text{A}}V_{\text{s}}$, where V_{s} is the swollen volume of the latex particle and N_{A} is the Avogadro constant. The entering radical will have degree of polymerization z, which if it arises directly from an ionic initiator such as persulfate might be $z \approx 3$, while if this entering radical is one which has undergone exit (desorption) from another particle, then $z = 1$.[9,35,36] The probability of an entering z-mer propagating to a j-mer without undergoing termination is then

$$P_j = \prod_{i=z}^{j} \frac{k_{\text{p}}^{i}[\text{M}]_{\text{p}}}{k_{\text{p}}^{i}[\text{M}]_{\text{p}} + \dfrac{k_{\text{t}}^{i\text{L}}}{N_{\text{A}}V_{\text{s}}}} \quad (5)$$

There is experimental evidence[21,28,37] that the termination rate coefficient (at least above c^{**}) can be estimated assuming a diffusion-controlled (Smoluchowski) expression

$$k_{\text{t}}^{i\text{L}} = 4\pi D^{i\text{L}} p^{i\text{L}} \sigma N_{\text{A}} \quad (6)$$

where $D^{i\text{L}}$ is the relative diffusion coefficient for an i-meric radical and a long radical and $p^{i\text{L}}$ is the probability that they will undergo termination when within a distance σ; $p^{i\text{L}}$ takes account of the fact that radicals must be of opposite spin to undergo termination. The value of the diffusion coefficient can be approximated by that for the i-mer, comprising the sum of center-of-mass and reaction−diffusion terms:[27]

$$D^{i\text{L}} = D_i^{\text{com}} + D^{\text{rd}} \quad (7)$$

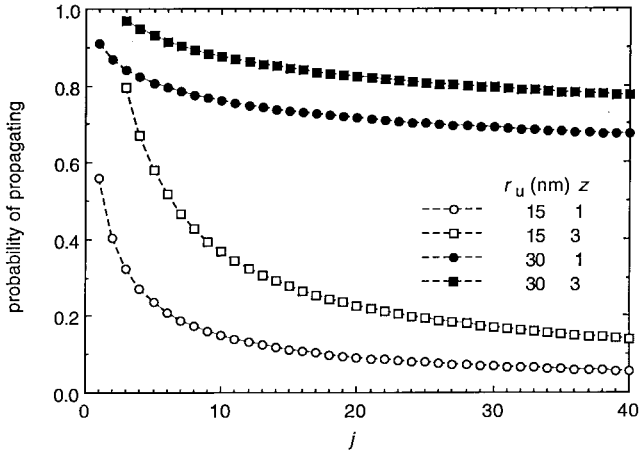

Figure 1. Cumulative probability of an entering radical propagating to a degree of polymerization j without terminating with a preexisting radical, for butyl acrylate seeded emulsion polymerization at 50 °C, for two different values of the unswollen particle radius r_u and for the degree of polymerization of the entering radical, z.

The reaction−diffusion term is found by[38] $D^{rd} = k_p[M]_p a^2/6$, where a is the root-mean-square end-to-end distance per square root of the number of monomer units in a polymer chain; evaluation of the two components of the overall diffusion coefficient shows that, even for a monomer which propagates as quickly as butyl acrylate,[2,39] the reaction−diffusion component is unimportant for regions of interest in the present study.

Designing a Zero−One Butyl Acrylate System. We now turn to the design of a butyl acrylate seeded system which should show zero−one kinetics, using the theory above. The propagation rate coefficient has been found by pulsed-laser polymerization,[2,39] and fits

$$k_p/\mathrm{dm^3\ mol^{-1}\ s^{-1}} = 1.8 \times 10^7 \exp(-17.4\ \mathrm{kJ\ mol^{-1}}/RT) \quad (8)$$

We take all k_p^i to be the same. The value of $[M]_p$ in the presence of monomer droplets was measured as described below as $[M]_p^{sat} = 5.7$ mol dm^{-3}.The center-of-mass component of the diffusion coefficient, D_i^{com}, at a given weight-fraction of polymer, w_p, was estimated using the experimentally determined scaling relationship for butyl methacrylate oligomers at 40 °C:[40]

$$D_i^{com}(w_p)/\mathrm{cm^2\ s^{-1}} = \frac{1.69 \times 10^{-5} - 4.5 \times 10^{-5} w_p + 3.72 \times 10^{-5} w_p^2}{i^{(0.664 + 2.02 w_p)}}, \quad 0.1 \le w_p \le 0.4 \quad (9)$$

The value of p^{iL} was taken as $^1/_4$,[25,37,41] while that for σ was taken as 7 nm. The value of z for a radical arising directly from persulfate (which is a species such as $^\bullet M_3SO_4^-$, where M is a monomer unit) was taken as its greatest likely value, $z = 3$,[35,36,42] while that for a reentering radical derived from the exit was taken as $z = 1$ (such radicals arise from transfer within the particle and are thus hydrophobic).

The results of calculating the cumulative probability of propagating to a degree of polymerization j inside the particle without terminating are shown in Figure 1, for two seed particles with unswollen radii 15 and 30 nm; the swollen and unswollen radii are trivially related by mass balance, given the value of $[M]_p$.[9] It can be seen that very little growth to moderate degrees of polymerization is expected for the smaller of these two sizes, whereas that is not the case for the larger. These calculations suggest that zero−one conditions would be expected to be an adequate approximation for the kinetics of growth of a BA seed at 50 °C with unswollen radius 15 nm but not for particles that are much larger than this. The small activation energies of BA for propagation (18 kJ mol^{-1}) and termination (which is essentially diffusion-controlled) suggest that this size criterion should be applicable over a moderate temperature range.

Contrary to the inference just given, Zirkzee *et al.*[43] have suggested that BA seeded emulsion polymerizations may follow zero−one kinetics (at 20 °C with a redox initiator) for particle radii as large as 65 nm. However, this conclusion was based on being able to fit observed rate data to zero−one kinetics, which is a necessary but not sufficient condition for the system to be zero−one.

It is essential to be able to provide experimental evidence that the conditions chosen here indeed do give zero−one kinetics. Another necessary but not sufficient condition is that the value of $\bar{n}$, the average number of radicals per particle, should not exceed $^1/_2$. A sufficient condition is that the polymerization rate in interval 2 (i.e., emulsion polymerization in the presence of monomer droplets, when $[M]_p$ is essentially constant throughout the interval) be constant, provided that $\bar{n}$ is less than $^1/_2$. The reason for this being a sufficient condition[8] is that a system is zero−one only if termination is not rate-determining; if termination were to be rate-determining, then as the swollen particle volume increases during interval 2 polymerization, the *termination rate* would decrease if $\bar{n}$ is low (since this rate is proportional to V_s^{-1}—see text preceding eq 5), which would lead to a small but significant decrease in the *overall* polymerization rate. Thus seeing a constant rate in interval 2 will show conclusively that a system is zero−one.

Experimental Section

The seed latex was composed of polystyrene with a radius of 15 nm, kindly provided by BASF (recipes for particles with this size have been given elsewhere[44]); particle size was measured by ultracentrifugation. The same technique gave limited information on the polydispersity, which was estimated as approximately 1.15. The particle number density used was 8×10^{17} dm^{-3} (giving an initial solids content of about 1%). The method requires that no secondary particle formation or coagulation occur; this was checked for each run using capillary hydrodynamic fractionation (CHDF).

Rates were measured by both dilatometry and by gravimetry. Dilatometry was performed in a 60 mL jacketed dilatometer, using a water bath for temperature control. Seed, monomer, surfactant, and degassed water were mixed together and stirred for at least 3 h. The dilatometer was then heated at the desired temperature, the initiator solution was added (typically 1 mL) as well as extra water to fill the dilatometer volume, the capillary was installed and filled with decane, and conversion was followed by an automatic tracking device. The final conversion was then measured by gravimetry, and the conversion vs time was calculated using the final conversion and the dilatometer contraction data.

Butyl acrylate monomer (Aldrich) was filtered through basic silica, distilled under reduced pressure at about 70 °C before use, and stored at 4 °C. A different batch of BA was prepared by partial bulk polymerization with benzoyl peroxide as initiator at 70 °C and subsequent reduced-pressure distillation at room temperature; this "polymerization distillation" is a

Table 1. Experimental Conditions for All Runs, Where Reaction Rates (As d*x*/d*t*, Where *x* Is Fractional Conversion) and Values of $\bar{n}$ in Interval 2 Are Also Shown

experiment	temp, °C	KPS, mmol dm^{-3}	init. mass of PS seed, g	init. mass of BA, g	particle no., dm^{-3}	AMA, g	d*x*/d*t* s^{-1}	$\bar{n}$
			Dilatometry [60 mL]					
D25	50.0	0.63	0.75	2.22	8.3×10^{17}	0.28	0.0010	0.0012
			Gravimetry/Sampling [90 mL]					
DS11	50.9	0.69	1.04	3.53	7.7×10^{17}	0.27	0.0010	0.0015
DS12	60.6	0.69	1.04	3.49	7.7×10^{17}	0.33	0.0024	0.0029
DS13	71.8	0.69	1.08	3.28	8.0×10^{17}	0.29	0.0035	0.0031
DS14	56.0	0.62	1.08	3.00	7.9×10^{17}	0.30	0.0012	0.0013
DS17	60.2	0.63	1.04	2.67	7.7×10^{17}	0.25	0.0021	0.0019
DS19	69.5	0.10	1.06	2.73	7.8×10^{17}	0.35	0.0020	0.0016
DS24	65.4	0.63	1.04	2.95	7.7×10^{17}	0.40	0.0025	0.0024

technique which eliminates impurities which may interfere with the kinetics and which have a boiling point similar to that of the monomer.[45] Samples of BA purified by these alternate techniques did not show any differences in their kinetics or MWD. Potassium persulfate (KPS, Univar) was used as initiator and hydroquinone as inhibitor. Both were used without further purification. The additional surfactant used was Aerosol MA 80 (AMA, sodium dihexyl sulfosuccinate, National Starch & Chemical).

The seeded emulsion runs, where samples were taken, were performed in a 90 mL sidearm jacketed dilatometer. Seed, monomer, surfactant, and degassed water were mixed together and stirred for at least 3 h before heating the mixture to the desired temperature. The initiator solution was then added (1.5 mL) and the first sample taken (nil conversion). Monitoring temperature on-line and looking for the small exotherm provided the necessary information as when to start sampling. Samples were taken with a pipet (approximately 1−1.5 g) and rapidly transferred to a vial which was then sealed and cooled in ice. The solids content and hence the conversion were then determined gravimetrically on these samples. Dilatometry was used for one run to examine the rate with good accuracy; samples for MWDs were obtained from systems wherein conversion was obtained from these samples by gravimetry, where the rate data are of course less accurate.

The saturation concentration ($[M]_p^{sat}$) of BA in the PS seed was measured using a 90 mL sidearm dilatometer. Seed and monomer were mixed in similar amounts as used for the kinetics and stirred for about 24 h. A capillary was then set on top of the dilatometer and water injected through the dilatometer arm with a syringe so that the capillary was filled. Excess monomer was then allowed to cream in the capillary, and its amount was measured (knowing the capillary diameter). The amount of monomer dissolved in the particles can then be calculated, giving $[M]_p^{sat} = 5.7$ mol dm^{-3}. The amount of monomer dissolved in the aqueous phase was neglected in this procedure; the error induced by this is small, since the saturated monomer concentration in the water phase is ca. 6×10^{-3} mol dm^{-3},[46] and with a solids content of about 10%, about 99% of the monomer is located in particles at the onset of saturation.

Details of all runs are shown in Table 1. The value of $\bar{n}$ was obtained from the observed rate (as d(fractional conversion)/d*t*, d*x*/d*t*) using the measured value of the monomer concentration and eq 8, together with the relation

$$\frac{dx}{dt} = \frac{k_p[M]_p \bar{n} N_c}{n_M{}^0 N_A} \qquad (10)$$

where $n_M{}^0$ is the initial number of moles of monomer present per unit volume of water in the reactor and N_c is the number concentration of particles.

In a kinetic study involving fast exothermic reaction, good temperature control is essential. A typical temperature profile of an experiment is shown in Figure 2. The initial drop in temperature is caused by the introduction of the initiator while the subsequent temperature rise is due to the polymerization reaction. The inhibition time (between initiator introduction and the reaction start) depends on the initiator concentration and the reaction temperature. For conditions of slow reaction, nitrogen bubbling was used to shorten the inhibition time. Figure 2 shows the maximum temperature increase, observed for the fastest reaction and, consequently, the shortest inhibition time. The temperature rises observed were between about 0.2 and 1.2 °C and can be considered as negligible, as far as the kinetics is concerned. The similarities of the observed rates obtained by both gravimetry and dilatometry (Table 1) suggest that the small exotherm does not lead to significant error in the steady-state rate measured dilatometrically.

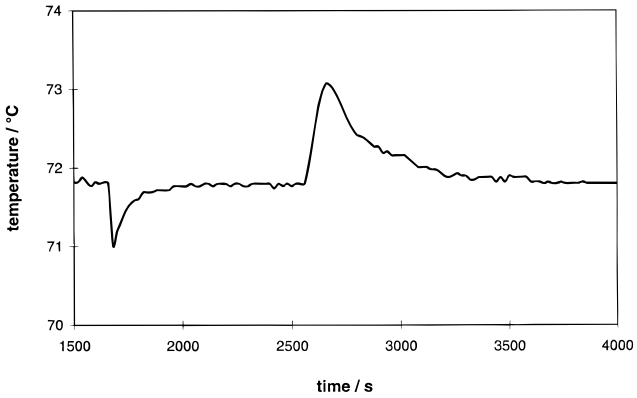

Figure 2. Temperature profile of run DS13.

The method requires that the slope of ln *P*(*M*) be unaffected by spontaneous (background thermal) polymerization; earlier work has shown that such polymerization can be significant in butyl acrylate.[46] To check this effect in the present system, a seeded run was carried out in the absence of added KPS initiator. The polymerization rate so obtained was a factor of 15 less than the lowest rate observed under the same conditions in the presence of KPS, suggesting that spontaneous polymerization will not affect the slope of ln*P*(*M*) in the present system.

Samples for GPC samples were prepared by dissolution of the polymers in tetrahydrofuran (THF) and filtered after about 24 h. Concentrations of about 1 mg mL^{-1} were used. The chromatographic system used in this work (Waters) was equipped with four columns (Waters, size 10^6, 10^5, 10^4, and 10^3 Å) and a Waters Model 410 refractive index detector. THF was used as the eluent at a flow rate of 0.8 cm^3 min^{-1}. PS standards (12 standards, Waters and Polymer Laboratories; molecular weights between 6.85×10^6 and 4×10^3) were used for calibration, with the "universal" calibration method being used for BA.[47]

Results

Rate Data. All BA seeded emulsion polymerizations started in interval 2 (polymerization in the presence of monomer droplets) and went over to interval 3 (absence of monomer droplets). All runs showed an inhibition period, followed by a nonstationary reaction start (up to about 10−15% conversion), an extensive interval 2

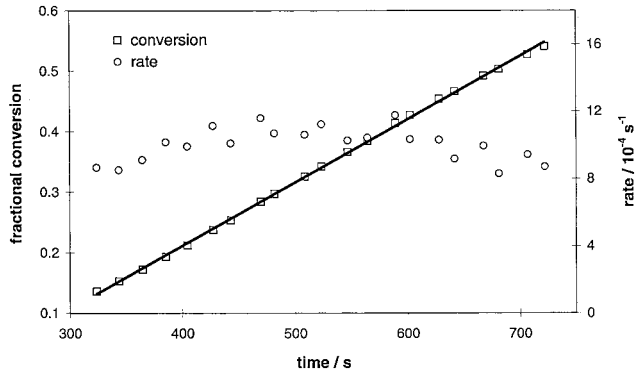

Figure 3. Conversion and reaction rate as a function of time for the interval 2 part of a BA seeded run (number D25) at 50 °C.

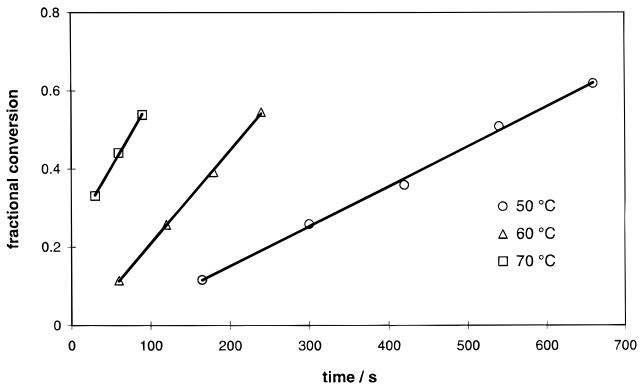

Figure 4. Effect of changes in temperature on conversion. Data were obtained gravimetrically.

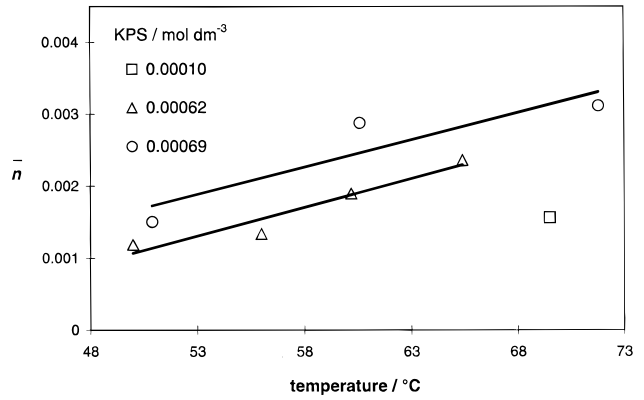

Figure 5. Effect of changes in initiator concentration on $\bar{n}$. Data were obtained gravimetrically.

(up to about 60% in our experimental conditions), and an interval 3 regime. Figure 3 shows conversion and reaction rate as a function of time for the Interval 2 part of a BA seeded run at 50 °C. It can be seen from this figure that the constant reaction rate, on a 50% conversion scale, satisfies the sufficient condition for the system to be a zero−one system. Table 1 shows the reaction rates and interval 2 values of $\bar{n}$. Figures 4 and 5 show the influence of initiator concentration and temperature on rate and on $\bar{n}$. These figures show that the variation of rate with temperature and initiator concentration implies an increase of $\bar{n}$ with radical flux, consistent with our neglect of thermal entry.

MWD Data. The method requires the MWD corresponding to the seed to be subtracted from that of the samples. As can be seen in Figure 6, the seed PS and the poly(BA) formed during the seeded run show widely

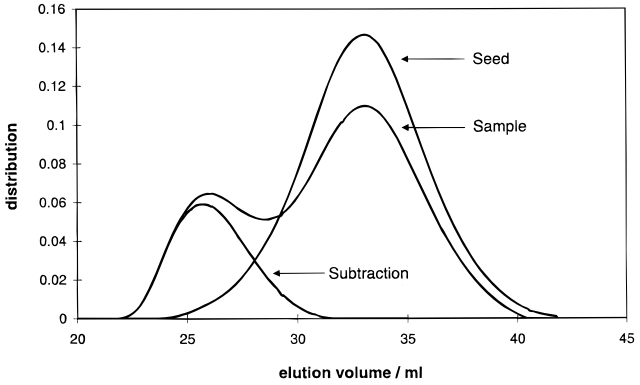

Figure 6. GPC distributions for run DS13, at 33.1% fractional conversion, showing seed, MWD after second-stage growth, and MWD of the polymer formed by second-stage growth, obtained by subtraction of an appropriately normalized[21] seed distribution.

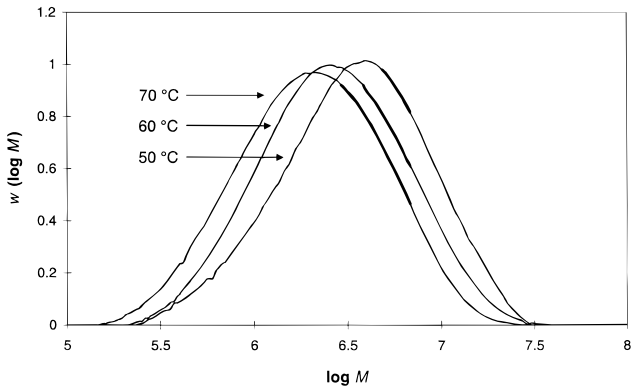

Figure 7. GPC distributions for polyBA formed in runs DS11, DS12, and DS13. The regions over which the slope were measured for use in eq 1 are shown as bold lines.

different distributions, the poly(BA) being in the high molecular weight region, whereas the PS lies in the low molecular weight region. This results in an easy subtraction, the high molecular region of the poly(BA) being virtually unaffected by this operation. The residual signal, positive or negative, resulting from an imperfect seed subtraction (in the low molecular weight region) was then set to zero.

The resulting distribution for the formed polyBA was then used for the MWD calculation. The Mark−Houwink parameters used to compute the MWD were[2] K/dL g^{-1} = 11.4 × 10^{-5} (PS) and 12.2 × 10^{-5} (polyBA), and a = 0.716 (PS) and 0.700 (polyBA).

Figure 7 shows the GPC distributions, w(log M), for three pBA samples produced at 50, 60 and 70 °C, with the corresponding ln $P(M)$ in Figure 8; the jagged nature of the curves at very low log M is due to baseline subtraction. It is apparent that the ln $P(M)$ vs M curves are by no means linear in M, an observation which has been made elsewhere.[6,7,13,21,28] The general trend was that higher polymerization temperatures produce more nonlinear ln $P(M)$ plots. There has been considerable discussion[6,7,13,21,28] as to the origins of this nonlinearity, e.g., effects arising from small impurities, termination, chain-branching, etc. The model calculations of Figure 1 indeed suggest that termination involving chains of moderate degree of polymerization may be a significant contribution. However, it has been shown that consistent results for transfer constants can be obtained by taking the slope of ln $P(M)$ in the region between the peak molecular weight and $\langle M_w \rangle$.[7,13] It is essential

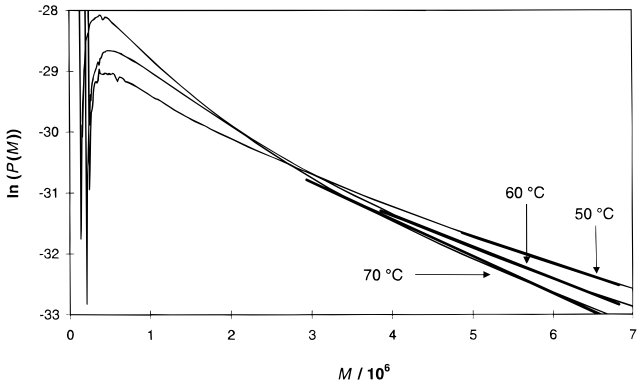

Figure 8. Data of Figure 7 converted to number MWD, displayed as ln $P(M)$. The regions over which the slope was measured for use in eq 1 are shown as bold lines.

to note that the ln $P(M)$ method is only valid providing the linear region is chosen suitably, since otherwise very misleading results can be obtained.[7,13,28] The most important criterion in the choice of this region is that it should include $\langle M_w \rangle$ and that there be enough polymer present in that region for a reliable signal: for example, trying to find an apparent linear region at very high molecular weights can lead to erroneous results, since there is very little polymer formed at very high molecular weight and hence the GPC signal, being proportional to $P(M)/M^2$, can be very prone to error after baseline subtraction. In the present case, a good linear region was found between $\langle M_w \rangle$ and the calibration limit of the standards; these are shown as bold lines in Figures 7 and 8. It is apparent from Figure 7 that there is extensive polymer in this region. This region is well outside the exclusion limit of the columns, which is about 10^7.

Table 2 summarizes the GPC results ($\langle M_w \rangle$, $\langle M_n \rangle$, the polydispersity $\gamma = \langle M_w \rangle / \langle M_n \rangle$), and the slope of the ln $P(M)$ as well as the conversions for all samples.

The MWD for polyBA all showed a very high molecular weight, often with $\langle M_w \rangle$ close to or beyond the exclusion limit of our system. A combination of this effect and the effect of a significant part of the measured distributions being outside the calibration domain results in inaccurate values for $\langle M_w \rangle$ and $\langle M_n \rangle$. Nevertheless, the collection of these data shown in Figure 9 shows a clear trend, the molecular weight strongly decreasing as temperature increases. In addition, the initiator concentration used for the seeded run does not influence the resulting molecular weight. This indeed suggests that chain-stopping in our system is transfer dominated.

An Arrhenius plot of the transfer constant C_M from these data is presented in Figure 10. For each temperature, the scatter observed for the ln C_M values does not show any trend with sample conversion or initiator concentration. This again supports the hypothesis that the linear part of these ln$P(M)$ arises entirely from stoppage by transfer to monomer. These data can be fitted by

$$C_M = (0.016 \pm 0.003) \exp(-(15.2 \pm 0.6) \text{ kJ mol}^{-1}/RT) \quad (11)$$

The corresponding 95% confidence interval for this Arrhenius fit (using code kindly supplied by Dr. A. van Herk[48]) is shown in Figure 11.

Table 2. Conversion and GPC Results for Formed PolyBA

experiment	sample conversion, %	$\langle M_w \rangle$	$\langle M_n \rangle$	γ	slope of ln $P(M)$ $\times 10^7$
DS11	11.6	4.84×10^6	2.17×10^6	2.2	−4.33
	25.9	4.98×10^6	2.36×10^6	2.1	−4.32
	35.9	4.45×10^6	2.35×10^6	1.9	−4.49
	61.8	4.67×10^6	2.22×10^6	2.1	−4.38
DS14	8.5	3.75×10^6	1.47×10^6	2.5	−5.09
	18.5	4.26×10^6	1.52×10^6	2.8	−4.82
	29.7	4.06×10^6	1.49×10^6	2.7	−4.95
	40.9	4.35×10^6	1.51×10^6	2.9	−4.75
	52.1	4.29×10^6	1.58×10^6	2.7	−4.92
DS12	11.4	3.81×10^6	1.86×10^6	2.0	−5.23
	25.7	3.77×10^6	1.75×10^6	2.2	−5.21
	39.2	3.58×10^6	1.64×10^6	2.2	−5.30
	54.6	3.25×10^6	1.42×10^6	2.3	−5.33
DS17	8.60	3.51×10^6	1.75×10^6	2.0	−5.44
	22.1	3.59×10^6	1.64×10^6	2.2	−5.40
	34.2	3.50×10^6	1.57×10^6	2.2	−5.41
	47.0	3.52×10^6	1.53×10^6	2.3	−5.40
	56.0	3.55×10^6	1.47×10^6	2.4	−5.44
DS24	15.1	3.22×10^6	1.39×10^6	2.3	−5.74
	23.1	3.37×10^6	1.31×10^6	2.6	−5.57
	32.0	3.32×10^6	1.21×10^6	2.8	−5.51
	37.2	3.37×10^6	1.20×10^6	2.8	−5.42
	42.1	2.72×10^6	1.03×10^6	2.6	−5.93
	46.2	3.31×10^6	1.13×10^6	2.9	−5.52
DS13	33.1	2.91×10^6	1.36×10^6	2.1	−6.09
	44.1	2.80×10^6	1.25×10^6	2.2	−6.06
	53.9	2.48×10^6	1.18×10^6	2.1	−6.25
DS19	14.5	2.90×10^6	1.35×10^6	2.1	−6.17
	28.0	2.93×10^6	1.35×10^6	2.2	−6.09
	36.3	2.90×10^6	1.35×10^6	2.1	−6.04
	47.6	3.03×10^6	1.28×10^6	2.4	−5.93
	53.8	2.61×10^6	1.20×10^6	2.2	−6.22
	61.5	2.62×10^6	1.15×10^6	2.3	−6.08

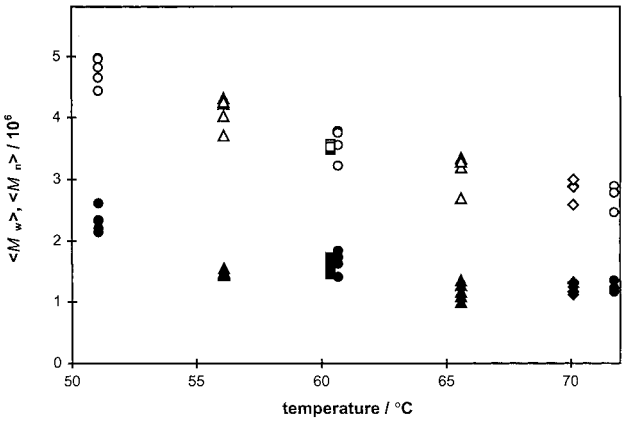

Figure 9. Data for $\langle M_w \rangle$ (open symbols) and $\langle M_n \rangle$ (closed symbols) for formed polyBA, with different initiator concentrations and temperatures: 0.69 mmol dm^{-3} (○), 0.10 mmol dm^{-3} (◇), and the two values for 0.63 mmol dm^{-3} KPS are for BA samples purified by distillation alone (△) and polymerization−distillation (□).

Another result for the transfer constant for BA monomer is that reported by Devon and Rudin[49] from studies of styrene/BA emulsion copolymerization at 60 °C. These authors inferred a value for C_M for BA monomer as 2.5×10^{-4}, which differs significantly from the value from eq 11, which is 7×10^{-5}. However, these authors inferred their transfer constant by modeling data in their system, where the highest mole fraction of BA was 65%; moreover, branching (which is likely for higher mole fractions of BA) was not considered in the data analysis. As stated earlier, the C_M results of Beuermann *et al.*[2] were inferred somewhat indirectly

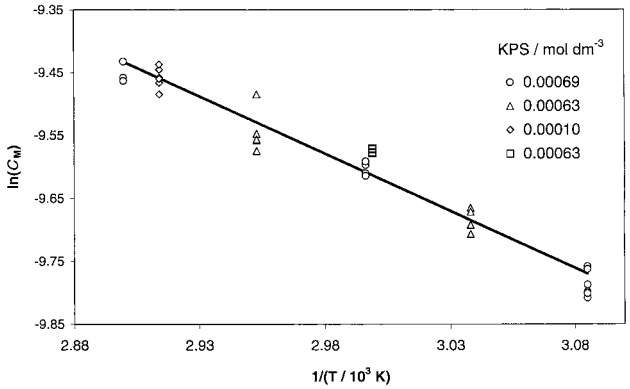

Figure 10. Arrhenius plot of transfer constant, from slopes of ln $P(M)$ data. The two values for 0.63 mmol dm^{-3} KPS are for BA samples purified by distillation alone (△) and polymerization−distillation (□).

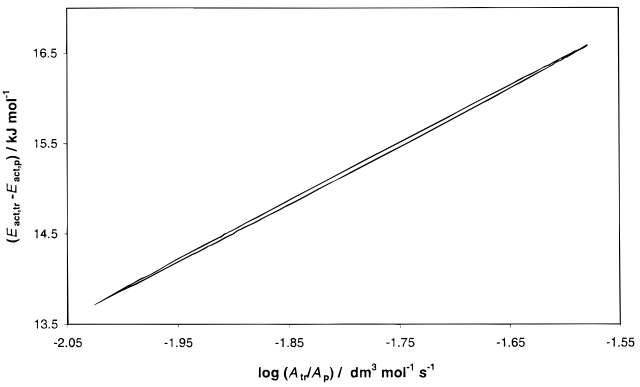

Figure 11. 95% confidence interval for the Arrhenius fit of Figure 10.

and implied that the activation energies for transfer and propagation are similar, a result which can be discounted on theoretical grounds. The present C_M values are therefore considered more reliable than either of these earlier results.

The transfer rate coefficient itself can then be estimated by using the PLP results for k_p, eq 8, yielding

$$k_{tr}/\mathrm{dm^3\ mol^{-1}\ s^{-1}} = (2.9 \pm 0.9) \times 10^5 \exp(-(32.6 \pm 0.8)\ \mathrm{kJ\ mol^{-1}}/RT) \quad (12)$$

The quoted uncertainties combine those for C_M and k_p.

The data obtained here for k_{tr} and for the steady-state $\bar{n}$ with chemical initiator (run D25) can be used to test models developed for entry and exit in zero−one emulsion polymerizations with ionic surfactants.[9,22,35] The final expression for $\bar{n}$ with these models is[9]

$$\frac{d\bar{n}}{dt} = \rho(1 - 2\bar{n}) - 2k_{tr}[M]_p \frac{k_{dM}\bar{n}}{k_{dM}\bar{n} + k_p^1[M]_p}\bar{n}; \qquad k_{dM} = \frac{3D_W}{r_s^2}\frac{C_W}{[M]_p} \quad (13)$$

where D_W and C_W are, respectively, the diffusion coefficient of monomeric radicals and concentration of monomer in the water phase. The cited model[35] for entry (propagation in the aqueous phase to a z-mer in competition with aqueous-phase termination, which then enters irreversibly) predicts essentially 100% initiator efficiency; i.e., $\rho = 2k_d[I]N_A/N_c$, where k_d is the initiator dissociation rate coefficient. Any reasonable parameter set for the entry model will always predict 100% efficiency for a monomer which propagates as quickly as BA, since rapid propagation to a z-mer means that there will be negligible aqueous-phase termination. Values of all parameters required to evaluate the entry and exit rate coefficients and hence $\bar{n}$ for BA under zero−one conditions are either given above or available in the literature.[9] The resulting calculated steady-state value of $\bar{n}$ for the conditions of run D25 is 0.033. This compares poorly with the observed value of $\bar{n} = 0.0012$. Possible reasons for this discrepancy are now considered.

(a) The discrepancy of a factor of 25 cannot be ascribed to uncertainties in the parameters used for the model: for example, changing k_p and k_{tr} by ±50% (a large estimate of the uncertainty in these quantities) results in an approximately a proportional change in the calculated $\bar{n}$ (including of course changing the experimental value as appropriate, since this is deduced from the experimental rate using a value of k_p).

(b) Another possible cause of this discrepancy between calculated and observed $\bar{n}$ is the wide particle size distribution (PSD) of the seed (it will be recalled that its polydispersity is approximately 1.15; i.e., its average size is about 15 nm with a width of about 6 nm. The models cited above for the dependence of the entry and exit rate coefficients on *size* were used (with techniques given elsewhere[9]) to calculate the overall rate in a system with a Gaussian PSD with mean radius 15 nm and standard deviation 6 nm; the resulting overall rate (where because of the different size dependences of entry and exit rate coefficients, the value of $\bar{n}$ depends on size) is then used to calculate two different average values of $\bar{n}$: the true average over all particle sizes and the average from the overall rate using the average particle radius. Using the parameters given above, the true average value of $\bar{n}$ is 0.016, while that calculated from the overall rate and average size is 0.033, as stated above. The value of $\bar{n}$ calculated from the full PSD is a factor of 2 smaller than that calculated from the average particle size, which is more consistent with the experimental result, but the discrepancy is still a factor of about 10. No further exploration of the possibility of the nonmonodisperse PSD accounting for this remaining discrepancy is possible until a more precise experimental PSD is available. This is difficult but not impossible for such small particles, and work in this direction is being pursued.

(c) A third possible explanation for the discrepancy is that the larger particles in this polydisperse seed follow pseudo-bulk kinetics more than they follow zero−one kinetics (of course, both zero−one and pseudo-bulk are limiting cases of a complete kinetic description,[9,10]) which unfortunately can at present only be simulated by laborious Monte Carlo methods such as that of Tobita[50]). If it is assumed that the present system is entirely pseudo-bulk, then the value of $\bar{n}$ can be calculated using a model for the full chain-length dependence of the termination rate coefficient,[25,26] with the requisite diffusion coefficients for monomeric and oligomeric radicals found from eq 9.[40]) This calculation yields $\bar{n} = 0.00013$, which is now an order of magnitude *lower* than experiment, while the zero−one treatment yields an order of magnitude higher. Since the model calculations based on eq 5 suggest that particles bigger than 15 nm will show significant non-zero−one behavior, it is possible that the tendency of larger particles in the

relatively broad seed to follow non-zero−one kinetics can provide a further contribution toward explaining the apparent discrepancy.

It is noted that having a significant component of the polymer formed under non-zero−one conditions (i.e., some chain stoppage by termination rather than transfer) will not invalidate the method used to infer C_M from experiment, because this method explicitly requires that the slope of the linear region of ln $P(M)$ be independent of radical flux; this can only happen if the chains of polymer in this region are stopped by transfer and not by termination.

Conclusions

The technique presented here for obtaining transfer constants represents a combination of methods which should be applicable for obtaining such data for "recalcitrant" systems: examining the full molecular weight distribution in a heteroseeded emulsion polymerization where the conditions have been designed to be zero−one, i.e., where entry leads to "instantaneous" termination. This obviates problems which can arise from contributions to the MWD from termination and from chain-branching to polymer.

The Arrhenius parameters for transfer to monomer for BA obtained here, $k_{tr}/dm^3\ mol^{-1}\ s^{-1} = 2.9 \times 10^5 \exp(-32.6\ kJ\ mol^{-1}/RT)$, are the first reported for acrylates. There are few data in the literature for comparison. Stickler and Meyerhoff[45] carried out meticulous studies of transfer to monomer in methyl methacrylate, by using rigorously purified monomer, and extremely low radical fluxes and by checking molecular weight distributions through average values obtained by both viscometry and light scattering. They report the temperature dependence of the transfer constant, which can be converted to transfer by using new values for the propagation rate coefficient of MMA from an IUPAC Working Party,[51] viz., $k_p/dm^3\ mol^{-1}\ s^{-1} = 10^{6.43} \exp(-22.36\ kJ\ mol^{-1}/RT)$; this yields $k_{tr}/dm^3\ mol^{-1}\ s^{-1} = 2.0 \times 10^5 \exp(-46.1\ kJ\ mol^{-1}/RT)$ for MMA. The frequency factor found in the present work for BA, $2.9 \times 10^5\ dm^3\ mol^{-1}\ s^{-1}$, is almost the same as that found for methyl methacrylate. The frequency factors for both monomers are consistent with each other, and both are significantly less than that for propagation (eq 8). Assuming that the transfer reaction involves hydrogen transfer,[31] this frequency factor suggests that the transition state is more hindered than the reactants,[3,30] presumably as the side chain in radical and/or monomer become restricted. The value of the activation energy for BA is not atypical: for example, gas-phase hydrogen-atom transfer reactions between ethyl radicals and alkenes[52] have activation energies in the range 25−35 kJ mol^{-1}, consistent with the BA transfer reaction involving a backbone hydrogen (not surprisingly, these same small-molecule gas-phase reactions have significantly greater frequency factors than that obtained here, viz., ca. $10^8\ dm^3\ mol^{-1}\ s^{-1}$). The correlation of the present data with theory,[3] including comparison with homologous methacrylate systems, is an important area for future investigation.

Acknowledgment. The support of the Swiss National Science Foundation and of the Australian Research Council are gratefully acknowledged. We appreciate the collaboration of BASF Kunstofflaboratorium who kindly supplied the styrene latex used as seed in this work.

References and Notes

(1) Brandrup, A.; Immergut, E. H. In *Polymer Handbook*, 3rd ed.; Brandrup, A., Immergut, E. H., Eds.; Wiley-Interscience: New York, 1989.
(2) Beuermann, S.; Paquet, D. A.; McMinn, J. H.; Hutchinson, R. A. *Macromolecules* **1996**, *29*, 4206.
(3) Heuts, J. P. A.; Sudarko; Gilbert, R. G. *Macromol. Symp.* **1996**, *111*, 147.
(4) Lovell, P. A.; Shah, T. H.; Heatley, F. *Polym. Commun.* **1991**, *32*, 98.
(5) Lovell, P. A.; Shah, T. H.; Heatley, F. In *Polymer Latexes—Preparation, Characterization and Applications*; Daniels, E. S., Sudol, E. D., El-Aasser, M., Eds.; ACS Symposium Series 492; American Chemical Society: Washington DC, 1992; p 188.
(6) Hutchinson, R. A.; Paquet, D. A.; McMinn, J. H. *Macromolecules* **1995**, *28*, 5655.
(7) Moad, G.; Moad, C. L. *Macromolecules* **1996**, *29*, 7727.
(8) Ballard, M. J.; Napper, D. H.; Gilbert, R. G. *J. Polym. Sci., Polym. Chem. Ed.* **1984**, *22*, 3225.
(9) Gilbert, R. G. *Emulsion Polymerization: A Mechanistic Approach*; Academic: London, 1995.
(10) Clay, P. A.; Gilbert, R. G. *Macromolecules* **1995**, *28*, 552.
(11) Christie, D. I.; Gilbert, R. G. *Macromol. Chem. Phys.* **1996**, *197*, 403.
(12) Schoonbrood, H. A.; Pierik, S. C. J.; van den Reijen, B.; Heuts, J. P. A.; German, A. L. *Macromolecules* **1996**, *29*, 6717.
(13) Suddaby, K. G.; Maloney, D. R.; Haddleton, D. M. *Macromolecules* **1997**, *30*, 702.
(14) Schweer, J.; van Herk, A. M.; Pijpers, R. J.; Manders, B. G.; German, A. L. *Macromol. Symp.* **1995**, *92*, 31.
(15) Schoonbrood, H. A. S.; German, A. L.; Gilbert, R. G. *Macromolecules* **1995**, *28*, 34.
(16) Lichti, G.; Gilbert, R. G.; Napper, D. H. *J. Polym. Sci. A* **1980**, *18*, 1297.
(17) Said, Z. F. M.; Hassan, S. A.; Dunn, A. S. In *Emulsion Polymers and Emulsion Polymerization*; Bassett, D. R., Hamielec, A. C., Eds.; ACS Symposium Series 165; American Chemical Society: Washington D. C., 1981; p 471.
(18) Kast, H.; Funke, W. *Makromol. Chem.* **1981**, *182*, 1553.
(19) Hawkett, B. S.; Napper, D. H.; Gilbert, R. G. *J. Chem. Soc., Faraday Trans. 1* **1980**, *76*, 1323.
(20) Shortt, D. W. *J. Liq. Chromatogr.* **1993**, *16*, 3371.
(21) Clay, P. A.; Gilbert, R. G.; Russell, G. T. *Macromolecules* **1997**, *30*, 1935.
(22) Casey, B. S.; Morrison, B. R.; Maxwell, I. A.; Gilbert, R. G.; Napper, D. H. *J. Polym. Sci. A: Polym. Chem.* **1994**, *32*, 605.
(23) Allen, P. E. M.; Patrick, C. R. *Makromol. Chem.* **1961**, *47*, 154.
(24) Benson, S. W.; North, A. M. *J. Am. Chem. Soc.* **1962**, *84*, 935.
(25) Scheren, P. A. G. M.; Russell, G. T.; Sangster, D. F.; Gilbert, R. G.; German, A. L. *Macromolecules* **1995**, *28*, 3637.
(26) Russell, G. T.; Gilbert, R. G.; Napper, D. H. *Macromolecules* **1993**, *26*, 3538.
(27) Russell, G. T.; Gilbert, R. G.; Napper, D. H. *Macromolecules* **1992**, *25*, 2459.
(28) Clay, P. A.; Christie, D. I.; Gilbert, R. G. In *Advances in Free-Radical Polymerization*; Matyjaszewski, K., Ed.; ACS Symposium Series 685; American Chemical Society: Washington DC, 1998; p 104.
(29) Lodge, T. P.; Muthukumar, M. *J. Phys. Chem.* **1996**, *100*, 13275.
(30) Heuts, J. P. A.; Radom, L.; Gilbert, R. G. *Macromolecules* **1995**, *28*, 8771.
(31) Moad, G.; Solomon, D. H. *The Chemistry of Free Radical Polymerization*; Pergamon: Oxford, England, 1995.
(32) Russell, G. T. *Macromol. Theory Simulations* **1995**, *4*, 497.
(33) Russell, G. T. *Macromol. Theory Simul.* **1995**, *4*, 519.
(34) Russell, G. T. *Macromol. Theory Simul.* **1995**, *4*, 549.
(35) Maxwell, I. A.; Morrison, B. R.; Napper, D. H.; Gilbert, R. G. *Macromolecules* **1991**, *24*, 1629.
(36) Gilbert, R. G. In *Emulsion Polymerization and Emulsion Polymers*; Lovell, P. A., El-Aasser, M. S., Eds.; Wiley: London, 1997; p 165.
(37) Fischer, H.; Henning, P. *Acc. Chem. Res.* **1987**, *20*, 200.
(38) Russell, G. T.; Napper, D. H.; Gilbert, R. G. *Macromolecules* **1988**, *21*, 2133.

(39) Lyons, R. A.; Hutovic, J.; Piton, M. C.; Christie, D. I.; Clay, P. A.; Manders, B. G.; Kable, S. H.; Gilbert, R. G. *Macromolecules* **1996**, *29*, 1918.
(40) Griffiths, M. C.; Strauch, J.; Monteiro, M. J.; Gilbert, R. G. *Macromolecules* submitted.
(41) Fischer, H. *Makromol. Chem.* **1966**, *98*, 179.
(42) Gilbert, R. G. In *Polymeric Dispersions. Principles and Applications*; Asua, J. M., Ed.; NATO Advanced Studies Institute; Kluwer Academic: Dordrecht, The Netherlands, 1997; p 1.
(43) Zirkzee, H. F.; Vandenenden, M. J. W. A.; Vankilsdonk, W. T.; van Herk, A. M.; German, A. L. *Acta Polym.* **1996**, *47*, 441.
(44) Morrison, B. R.; Casey, B. S.; Lacík, I.; Leslie, G. L.; Sangster, D. F.; Gilbert, R. G.; Napper, D. H. *J. Polym. Sci. A: Polym. Chem.* **1994**, *32*, 631.
(45) Stickler, M.; Meyerhoff, G. *Makromol. Chem.* **1978**, *179*, 2729.
(46) Maxwell, I. A.; Napper, D. H.; Gilbert, R. G. *J. Chem. Soc., Faraday Trans. 1* **1987**, *83*, 1449.
(47) Gallot-Grubisic, Z.; Rempp, P.; Benoit, H. *Polym. Lett.* **1967**, *5*, 753.
(48) van Herk, A. M. *J. Chem. Educ.* **1995**, *72*, 138.
(49) Devon, M. J.; Rudin, A. *J. Polym. Sci.: Part A: Polym. Chem.* **1986**, *24*, 2191.
(50) Tobita, H. *Macromolecules* **1995**, *28*, 5128.
(51) Beuermann, S.; Buback, M.; Gilbert, R. G.; Hutchinson, R. A.; Klumpermann, B.; Olaj, F. O.; Russell, G. T.; Schweer, J. *Macromol. Chem. Phys.* **1997**, *198*, 1545.
(52) Trotman-Dickenson, A. F.; Milne, G. S. *Tables of bimolecular gas reactions*; National Bureau of Standards: Washington DC, 1967; Vol. NSRDS-NBS 9.

MA9800515